

## Research article

[urn:lsid:zoobank.org:pub:E814BAB1-3B3D-4458-9F94-E1EF89191881](https://zoobank.org/pub:E814BAB1-3B3D-4458-9F94-E1EF89191881)

# *Litinium gludi* sp. nov. (Nematoda, Oxystominidae) from Kermadec Trench, Southwest Pacific Ocean

Daniel LEDUC<sup>1,\*</sup> & Zeng Qi ZHAO<sup>2</sup>

<sup>1</sup>National Institute of Water and Atmospheric Research (NIWA) Ltd, Wellington, New Zealand.

<sup>2</sup>Landcare Research, Private Bag 92170, Auckland Mail Centre, Auckland 1142, New Zealand.

\*Corresponding author: [Daniel.Leduc@niwa.co.nz](mailto:Daniel.Leduc@niwa.co.nz)

<sup>2</sup>Email: [Zhaoz@landcareresearch.co.nz](mailto:Zhaoz@landcareresearch.co.nz)

<sup>1</sup>[urn:lsid:zoobank.org:author:9393949F-3426-4EE2-8BDE-DEFFACE3D9BC](https://zoobank.org/author:9393949F-3426-4EE2-8BDE-DEFFACE3D9BC)

<sup>2</sup>[urn:lsid:zoobank.org:author:F5BEE9FD-801A-49C6-9585-C765EE77A123](https://zoobank.org/author:F5BEE9FD-801A-49C6-9585-C765EE77A123)

**Abstract.** Recent work on the taxonomy of nematodes in Southwest Pacific Ocean trenches has led to the discovery of taxa which so far appear to be restricted to the oceans' deepest environments. Here, *Litinium gludi* sp. nov. is described based on specimens obtained from a deep basin within the Kermadec Trench at 9540 m water depth. The new species differs from other species of the genus in having a conico-cylindrical tail, papillose labial sensilla, and heart- or leaf-shaped amphideal fovea. Both SSU and LSU phylogenetic analyses provide strong support for the placement of the new species within a clade containing both *Thalassoalaimus* and *Litinium*, and within Oxystomininae, which is consistent with the structure of the female reproductive system with only one posterior ovary in this subfamily. Our molecular analyses also indicate that the new species is most closely related to *Thalassoalaimus* despite lacking a caudal capsule, the main trait characterizing the latter genus, and despite being most morphologically similar to *Litinium*, particularly in the unusual shape of the amphideal fovea. However, given the changing definitions of the closely-related genera *Thalassoalaimus* and *Litinium* in recent years, available GenBank sequences may have been misidentified, which makes the interpretation of molecular phylogenetic analyses problematic. Given the current morphological definitions of *Litinium* and *Thalassoalaimus*, we choose to place the new species within *Litinium*, despite the apparently contradictory findings of molecular phylogenetic analyses. The placement of *Cricohalalaimus* in a clade with *Thalassoalaimus* and *Litinium* in both SSU and LSU analyses indicates that this genus should be placed within the Oxystomininae and not the Halalaiminae as in the current classification. This new proposed grouping is consistent with variation in the structure of the female reproductive system, a feature which appears more taxonomically informative than amphid shape for subfamily-level classification.

**Keywords.** Hadal, Oxystomininae, *Cricohalalaimus*, small subunit 18S rDNA, D2-D3 region of large subunit 28S rDNA.

Leduc D. & Zhao Z.Q. 2021. *Litinium gludi* sp. nov. (Nematoda, Oxystominidae) from Kermadec Trench, Southwest Pacific Ocean. *European Journal of Taxonomy* 748: 138–154. <https://doi.org/10.5852/ejt.2021.748.1347>

## Introduction

The Oxystominidae Chitwood, 1935 (order Enoplida Filipjev, 1929) is among the most common nematode families in deep-sea environments (Gambi *et al.* 2003; Bik *et al.* 2010a; Miljutin *et al.* 2010). This largely marine group is characterized by a thin elongated body, the outer labial and cephalic sensilla in separate circles, and the buccal cavity without teeth (Lorenzen 1981). The family includes three subfamilies: the Oxystomininae Chitwood, 1935, Halalaiminae De Coninck, 1965 and Paroxystomininae De Coninck, 1965, which are differentiated based on the amphid shape, the structure of the female reproductive system and the presence/structure of the precloacal supplements. The Oxystomininae comprises five genera, all of which except *Oxystomina* Chitwood, 1935 are exclusively marine; the presence of only the posterior ovary is considered a holapomorphy establishing the holophyly of the Oxystomininae (Lorenzen 1981). The Halalaiminae originally comprised a single genus, *Halalaimus* de Man, 1888, which is characterized by an elongated longitudinal amphideal aperture, an holapomorphic trait establishing the holophyly of the subfamily. The genus *Cricohalalaimus* Bussau, 1993 was later included in the subfamily by Smol *et al.* (2014) based on the similar structure of the amphideal aperture; this genus, however, is also characterized by the presence of a single posterior ovary in females, a feature of the Oxystomininae. There is no holapomorphy for the Paroxystomininae, which comprises *Paroxystomina* Micoletzky, 1924 and *Maldivea* Gerlach, 1962 (Lorenzen 1981). Phylogenetic analyses based on SSU sequences do not provide support for the monophyly of the Oxystomininae or Halalaiminae (Bik *et al.* 2010a), and no molecular sequences are yet available for the Paroxystomininae.

The majority of marine free-living nematode genera have wide water depth distributions spanning both coastal and deep-sea environments (> 200 m water depth), but some are mostly found in the deep sea (e.g., *Acantholaimus* Allgén, 1933, *Metasphaerolaimus* Gourbault & Boucher, 1981), while others are found exclusively in continental slope and/or deeper environments (e.g., *Bathyeurystomina* Lamshead & Platt, 1979, *Thelonema* Bussau, 1993, *Manganonema* Bussau, 1993). Phylogenetic analyses based on SSU data suggest repeated and recent interchanges between the deep sea and shallow water environments, with habitat transitions thought to be frequent for free-living nematodes (Bik *et al.* 2010b). In *Halalaimus* and *Oxystomina*, shallow water species appear to have evolved from deep water ancestors (Bik *et al.* 2010b); however, within the Oxystominidae, *Cricohalalaimus* Bussau, 1993 is the only genus with a distribution strictly restricted to the deep sea.

Limited core sampling has been conducted in hadal trenches to date (> 6000 m water depth), resulting in scant knowledge of nematode systematics in the deepest parts of the world's oceans. Taxonomic work on Tonga and Kermadec trench material has led to the discovery of new species and genera which so far appear to be restricted to hadal environments (Leduc 2015, 2016). More recently, sampling within the deep Kermadec Trench axis provided core samples from the trench's deepest basins, and the examination of specimens from a site located at 9540 m depth led to the discovery of a species of nematode, *Litinium gludi* sp. nov., which is described here. Phylogenetic relationships of this new species within the Oxystominidae are investigated using SSU and D2-D3 of LSU rDNA sequences.

## Material and methods

### Study area and sampling

The Kermadec Trench extends from approximately from 26 to 36°S near the northeastern tip of New Zealand's North Island, Southwest Pacific Ocean. Sediment samples were obtained from the deep axis of Kermadec Trench at 9540 m depth during *RV Tangaroa* cruise TAN1711 in December 2017. Sediments were obtained using a USNEL-type box corer (dimensions: 0.5 × 0.5 × 0.5 m, 0.125 m<sup>3</sup> capacity). Subsamples were obtained using a cut-off syringe with 29 mm internal diameter to a depth of 10 cm. Subsamples for morphological analyses were sliced into 1 cm layers and fixed in 10% buffered formalin. Nematodes were extracted from the remaining sediments by Ludox flotation and transferred to pure

glycerol (Somerfield & Warwick 1996). Species descriptions were made from glycerol mounts using differential interference contrast microscopy and drawings were made with the aid of a camera lucida. Measurements were obtained using an Olympus BX53 compound microscope with cellSens Standard software for digital image analysis.

Subsamples for molecular analyses were obtained as described above but the samples were frozen at  $-80^{\circ}\text{C}$  instead of being fixed in formalin. In the laboratory, frozen sediment samples were thawed overnight, then sieved through a  $20\ \mu\text{m}$  mesh to retain nematodes. Nematodes were extracted using the Ludox flotation method (Somerfield & Warwick 1996) and sorted under a dissecting microscope. One juvenile *Litinium gludi* sp. nov. specimen was isolated and transferred to a temporary slide to confirm its identity. This specimen was identified based on the characteristic shape of the cephalic region, cephalic sensilla, amphids, and tail.

All measurements are in  $\mu\text{m}$  (unless otherwise stated), and all curved structures are measured along the arc. Type specimens are held in the NIWA Invertebrate Collection, Wellington, New Zealand.

#### List of abbreviations

- a = body length/maximum body diameter
- b = body length/pharynx length
- c = body length/tail length
- c' = tail length/anal or cloacal body diameter
- cbd = corresponding body diameter
- L = total body length; n, number of specimens
- V = vulva distance from anterior end of body
- %V =  $V/\text{total body length} \times 100$

#### DNA extraction, PCR and sequencing

Following observation under a compound microscope, the specimen was transferred to lysis buffer and kept frozen at  $-80^{\circ}\text{C}$  prior to molecular analyses. DNA was extracted by the method of Zheng *et al.* (2002) with minor modifications (i.e., the nematode was not cut prior to being transferred to the lysis buffer solution). The DNA extract was stored at  $-20^{\circ}\text{C}$  until used as PCR template.

Primers for LSU amplification were forward primer D2A (5' ACAAGTACCGTGAGGGAAAAGT 3') and reverse primer D3B (5' TGCGAAGGAACCAGCTACTA 3') (Nunn 1992). Primers for the rDNA small subunit (SSU) were the forward primer 1096F, 5'-GGTAATTCTGGAGCTAATAC-3' and reverse primer 1912R, 5'-TTTACGGTCAGAACTAGGG-3' (first fragment), and the forward primer 1813F, 5'-CTGCGTGAGAGGTGAAAT-3' and reverse 2646R, 5'-GCTACCTTGTTACGACTTTT-3' (second fragment) (Holterman *et al.* 2006). For both SSU and LSU, the  $20\ \mu\text{l}$  PCR contained  $10\ \mu\text{l}$  REDExtract-N-Amp PCR ReadyMix (Sigma-Aldrich, USA),  $1\ \mu\text{l}$  ( $5\ \mu\text{M}$ ) each of forward and reverse primers, and  $2\ \mu\text{l}$  of DNA template. The thermal cycling program was as follows: denaturation at  $95^{\circ}\text{C}$  for 3 min, followed by 40 cycles of denaturation at  $94^{\circ}\text{C}$  for 15 s, annealing at  $55^{\circ}\text{C}$  for 30 s, and extension at  $72^{\circ}\text{C}$  for 30 s. A final extension was performed at  $72^{\circ}\text{C}$  for 7 min. The amplicons were electrophoresed on 1% TAE-agarose gel stained with SYBR<sup>®</sup> Safe, observed under UV illumination using the Gel-Doc system (BioRad, Hercules, CA, USA), and images processed using the Image Lab ver. 5.1 analysis software (BioRad). The PCR products were sequenced bi-directionally using the amplification primers by EcoGene (Auckland, New Zealand). Sequences were obtained with a 3500xL Genetic Analyzer (Applied Biosystems, USA) and assembled and edited with Sequencher ver. 4.10.1 (Gene Codes Corp.).

### Sequence alignment and phylogenetic inference

The ribosomal DNA SSU and LSU D2-D3 sequences were deposited in GenBank under accession numbers MW209715 and MW209714, respectively. The placement of the new SSU and D2-D3 of LSU sequences was investigated through a phylogenetic analysis of the representative genera of the Oxystominidae, as well as the Rhaptothyreidae Hope & Murphy, 1969 and Oncholaimoidea Filipjev, 1916, which have been shown to be closely related (Bik *et al.* 2010a; Leduc *et al.* 2018), and rooted using Ironidae de Man, 1876 sequences (all SSU sequences > 1300 bp except four ca 800 bp, and D2-D3 of LSU sequences > 600 bp).

DNA sequences were aligned using MUSCLE (Edgar 2004a, 2004b) with default parameters. Phylogenies were built in Geneious ver. 10.2.6 (<http://www.geneious.com>, Kearse *et al.* 2012). MrModelTest ver. 2.3 (Nylander 2004) in conjunction with PAUP\* ver. 4.0b10 (Swofford 2002) were used to select the best model using the Akaike Information Criterion. The substitution model [GTR (general time-reversible) + I (proportion of invariable sites) + G (gamma distribution)] was selected as the best-fit model for SSU alignments (1522 bp) and LSU alignments (722 bp), respectively. The trees were run with chain length of 1 100 000, and burn-in length of 100 000. The perimeter files from multiple runs were inspected for chain convergence in Tracer ver. 1.5 (Rambaut & Drummond 2007), and the trees were edited in FigTree ver. 1.4.2 (<http://tree.bio.ed.ac.uk/software/figtree>) and PowerPoint. These analyses were also conducted with PhyML ver. 3.0 using the default settings in Geneious ver. 10.2.6. The substitution model GTR, the NNI (default, fast) topology search and 1000 bootstrap replicates (Guindon *et al.* 2010) were selected for building the tree.

## Results

### *Systematics*

Phylum Nematoda Diesing, 1861  
Order Enoplida Filipjev, 1929  
Suborder Ironina Siddiqi, 1983  
Superfamily Ironoidea de Man, 1876

Family **Oxystominidae** Chitwood, 1935

#### **Diagnosis** (emended from Smol *et al.* 2014)

Body elongated and very thin at anterior end. Anterior sensilla in three separate circles, second and third circles clearly separated; inner labial sensilla papilliform or setiform, outer labial sensilla usually setiform (except in some species of *Litinium*), cephalic sensilla setiform. Buccal cavity narrow, tubular or funnel-shaped and without teeth. Sexual dimorphism in amphid shape sometimes present. Only orthometanemes with very short caudal filaments present. Pharynx inserts into body cuticle in region of buccal cavity; however, cephalic capsule not well developed. Posterior section of pharynx with undulating outline. Females didelphic-amphidelphic with antidromously reflexed ovaries or monodelphic-opisthodelphic. Males diorchic with opposed testes or only one anterior testis. Position of caudal glands variable.

Subfamily **Oxystomininae** Chitwood, 1935

#### **Diagnosis** (modified from Smol *et al.* 2014)

Only dorsolateral orthometanemes, ventral gland when present confined within pharyngeal region. Amphideal fovea and aperture variable but amphideal aperture never elongated, precloacal supplements (when present) papilliform, in single ventral row. Females monodelphic-opisthodelphic.

### Type genus

*Oxystomina* Filipjev, 1918

### Other valid genera

*Litinium* Cobb, 1920

*Nemanema* Cobb, 1920

*Thalassoalaimus* de Man, 1893

*Wieseria* Gerlach, 1956

### *Litinium* Cobb, 1920

#### Diagnosis (modified from Tchesunov *et al.* 2014)

Circles of six inner and six outer labial papillae ( $< 2 \mu\text{m}$ ) or setae ( $\geq 2 \mu\text{m}$ ) situated close together on anterior end, subapically, with circle of four cephalic papillae or setae posterior to circles of inner and outer labial sensilla. Amphideal fovea situated between circles of outer labial and cephalic sensilla. Amphideal fovea varies in shape between species and may differ in males and females of same species: may be ovoid with anterior round aperture, horseshoe-like or crescent contoured or more complex. Only one posterior antidromously reflexed ovary present; vulva shifted anteriorly. Tail never clavate, more or less short, cylindrical with rounded tip, occasionally conical or conico-cylindrical with pointed tip; terminal caudal capsule (thick cuticular lining at tip of tail) absent or weakly developed.

#### Remarks

The amphid of some species of *Litinium* Cobb, 1920 is described as being “horseshoe-shaped”. In the new species, our observations indicate that it is the superimposition of the amphideal aperture contour over the larger amphideal fovea contours that creates the appearance of a horseshoe-shaped structure. Whether this is also the case in other species of *Litinium* remains to be clarified.

There has been some confusion regarding the definitions of *Litinium* and *Thalassoalaimus*. The diagnoses provided by Smol *et al.* (2014) indicate that the two genera differ in the shape of the amphids (pocket-shaped amphideal fovea and slit-like aperture in *Thalassoalaimus* vs horseshoe- or heart-shaped fovea and round aperture in *Litinium*) and presence (*Thalassoalaimus*) or absence (*Litinium*) of a caudal capsule. However, we note that the pocket-shaped amphideal fovea and slit-like aperture in *Litinium subterraneum* Tchesunov, Mokievsky & Nguyen Vu Thanh, 2010 is identical to that of *Thalassoalaimus*. On the other hand, *Litinium profundorum* Tchesunov, Nguyen Vu Thanh & Nguyen Dinh Tu, 2014 has a weak thickening of the inner cuticle layer of the tail tip resembling a caudal capsule but is characterised by a horseshoe-shaped amphideal fovea typical of the genus *Litinium*. Most recently, Martelli *et al.* (2017) used the presence or absence of a caudal capsule as the sole distinguishing feature between the two genera, resulting in the transfer of several species of *Thalassoalaimus* to *Litinium*. Some of the newly transferred species, namely *L. aceratus* (Vitiello, 1970) Martelli, Lo Russo, Villares & Pastor de Ward, 2017 and *L. longicaudatus* (Vitiello, 1970) Martelli, Lo Russo, Villares & Pastor de Ward, 2017, as well as *L. gludi* sp. nov., are characterised by conico-cylindrical tails, which require the genus diagnosis of Tchesunov *et al.* (2014) to be emended. In addition, *L. longicaudatus*, *L. qangi* Tchesunov, Nguyen Vu Thanh & Nguyen Dinh Tu, 2014, *L. curticauda* Tchesunov, Nguyen Vu Thanh & Nguyen Dinh Tu, 2014 and *L. gludi* sp. nov. are characterised by papillose to short setose labial sensilla (0.5–2.5  $\mu\text{m}$  long), unlike all other species of the genus which have exclusively setose ( $\geq 2 \mu\text{m}$ ) labial sensilla.

### List of valid species

- L. abyssorum* Tchesunov, Nguyen Vu Thanh & Nguyen Dinh Tu, 2014  
*L. aceratus* (Vitiello, 1970) Martelli, Lo Russo, Villares & Pastor de Ward 2017  
*L. aequale* Cobb, 1920  
*L. australis* Martelli, Lo Russo, Villares & Pastor de Ward, 2017  
*L. bananum* Gerlach, 1956  
*L. curticauda* Tchesunov, Nguyen Vu Thanh & Nguyen Dinh Tu, 2014  
*L. dispariseta* Yu & Xu, 2018  
*L. egregius* (Steiner, 1916) Martelli, Lo Russo, Villares & Pastor de Ward 2017  
*L. gludi* sp. nov.  
*L. longicaudatus* (Vitiello, 1970) Martelli, Lo Russo, Villares & Pastor de Ward 2017  
*L. obtusilobus* Bussau, 1993  
*L. paramontemari* (Vitiello, 1970) Martelli, Lo Russo, Villares & Pastor de Ward 2017  
*L. parmatum* Wieser, 1954  
*L. pirum* (Lorenzen, 1969) Martelli, Lo Russo, Villares & Pastor de Ward 2017  
*L. profundorum* Tchesunov, Nguyen Vu Thanh & Nguyen Dinh Tu, 2014  
*L. quamgi* Tchesunov, Nguyen Vu Thanh & Nguyen Dinh Tu, 2014  
*L. setosus* (Timm, 1967) Martelli, Lo Russo, Villares & Pastor de Ward 2017  
*L. subterraneum* Tchesunov, Mokievsky & Nguyen Vu Thanh, 2010  
*L. volutum* Gerlach, 1962

### *Litinium gludi* sp. nov.

[urn:lsid:zoobank.org:act:FA79DFEF-A389-48AA-AF75-03984D69F202](https://zoobank.org/act:FA79DFEF-A389-48AA-AF75-03984D69F202)

Figs 1–4, Table 1

### Diagnosis

*Litinium gludi* sp. nov. is characterised by a slender body ( $a = 58\text{--}63$ ), a body length of  $895\text{--}1066\ \mu\text{m}$ , papilliform labial sensilla, short cephalic sensilla  $1.5\text{--}2.0\ \mu\text{m}$  or  $\sim 0.2$  cbd long, a large heart- or leaf-shaped amphideal fovea  $67\text{--}88\%$  cbd wide, a smaller amphideal aperture with two central longitudinal ridges, males with dimorphic sperm, spicules  $1.1\text{--}1.4$  times cloacal body diameter, a short and simple gubernaculum, and two precloacal setae.

### Differential diagnosis

The new species resembles *L. aceratus* and *L. longicaudatus*, the only other species of the genus with conico-cylindrical tails, and is particularly similar to *L. longicaudatus* in having papillose ( $< 2\ \mu\text{m}$ ) labial sensilla. *Litinium gludi* sp. nov. can be differentiated from *L. longicaudatus* by the shorter body ( $895\text{--}1066$  vs  $2180\text{--}2196\ \mu\text{m}$  in *L. longicaudatus*), lower 'a' ratio ( $58\text{--}63$  vs  $75\text{--}86$ ), and heart- or leaf-shaped amphideal fovea (vs pocket-shaped).

### Etymology

The species is named after Professor Ronnie Glud, leader of the HADES-ERC trench project and co-voyage leader.

### Material examined

#### Holotype

PACIFIC OCEAN • ♂; Kermadec Trench, voyage TAN1711, station 25, site 3;  $30.3815^\circ\text{S}$ ,  $176.6417^\circ\text{W}$ ; 9540 m water depth, 0–2 cm sediment depth; 3 Dec. 2017; NIWA 139257.

**Table 1.** Morphometrics ( $\mu\text{m}$ ) of *Litinium gludi* sp. nov.

	Males			Female paratype
	Holotype	Paratypes		
Specimen	M1	M2	M3	F1
L	1027	895	1066	930
a	60	60	63	58
b	5	4	5	5
c	11	10	11	10
c'	7.3	7.8	6.9	9.3
Body diam. at outer labial sensilla	6	6	6	6
Body diam. at cephalic setae	9	9	9	9
Body diam. at amphids	9	8	9	9
Length of cephalic sensilla	1.6–1.9	1.6–1.8	1.5–2.0	1.8
Amphideal fovea height	10	8	9	9
Amphideal fovea width	7	7	6	7
Amphideal fovea width/cbd (%)	78	88	67	78
Amphideal fovea from anterior end	4	5	4	5
Amphideal aperture height	7	6	6	6
Amphideal aperture width	3	3	3	3
Nerve ring from anterior end	85	77	87	83
Nerve ring cbd	17	15	17	16
Pharynx length	208	200	211	195
Pharyngeal diam. at base	12	9	11	10
Pharynx cbd at base	15	12	15	13
Max. body diam.	17	15	17	16
Spicule length	18	15	16	–
Gubernacular apophyses length	3	2	3	–
Cloacal/anal body diam.	13	12	14	10
Tail length	95	93	96	93
V	–	–	–	329
%V	–	–	–	35
Vulval body diam.	–	–	–	14

### Paratypes

PACIFIC OCEAN • 2 ♂♂, 1 ♀; Kermadec Trench, voyage TAN1711, station 25, site 3; 30.3815° S, 176.6417° W; 9540 m water depth, 0–2 cm sediment depth; 3 Dec. 2017; NIWA 139258.

### Description

#### Males

Body slender, cylindrical, widest at level of nerve ring, tapering slightly towards anterior extremity. Cuticle smooth, without ornamentation; somatic setae absent, except for sparse sublateral setae on tail. Cephalic region demarcated by slight constriction near posterior edge of amphideal fovea. Inner labial sensilla not observed; six outer labial papillae,  $\sim 0.5 \mu\text{m}$  long, located slightly anterior to amphideal fovea and four short cephalic sensilla, 1.5–2.0  $\mu\text{m}$  or  $\sim 0.2$  cbd long, situated far posteriorly at level of posterior edge of amphideal fovea. Amphideal fovea large, heart- or drop-shaped, with lightly cuticularized outline; amphideal aperture smaller, oval- or drop shaped, with two lightly cuticularized longitudinal central ridges spanning long axis of amphideal fovea. Buccal cavity narrow, cylindrical, with cuticularized portion 3–5  $\mu\text{m}$  deep. Pharynx muscular, cylindrical, surrounding posterior portion

of buccal cavity, widening towards posterior extremity but not forming true bulb. Nerve ring located slightly anterior to middle of pharynx. Secretory-excretory system not observed. Cardia 2–4  $\mu\text{m}$  long, partially embedded in intestine.

Reproductive system with two opposed and outstretched testes; anterior testis located to the left or right of intestine, posterior testis located on opposite side or on same side. Mature sperm in anterior testis large, elongated, 19–21  $\times$  2–3  $\mu\text{m}$ ; mature sperm in posterior testis smaller, globular, 1.5  $\times$  1.5–2.0  $\mu\text{m}$ . Spicules short, 1.1–1.4 times cloacal body diameter, curved distally, with ventrally bent capitulum. Gubernaculum small, simple, block-shaped, without lateral pieces, with poorly developed apophyses. Two precloacal papillae, 1.3–1.4  $\mu\text{m}$  long; posterior-most papilla located 11–14  $\mu\text{m}$  anterior to cloaca,

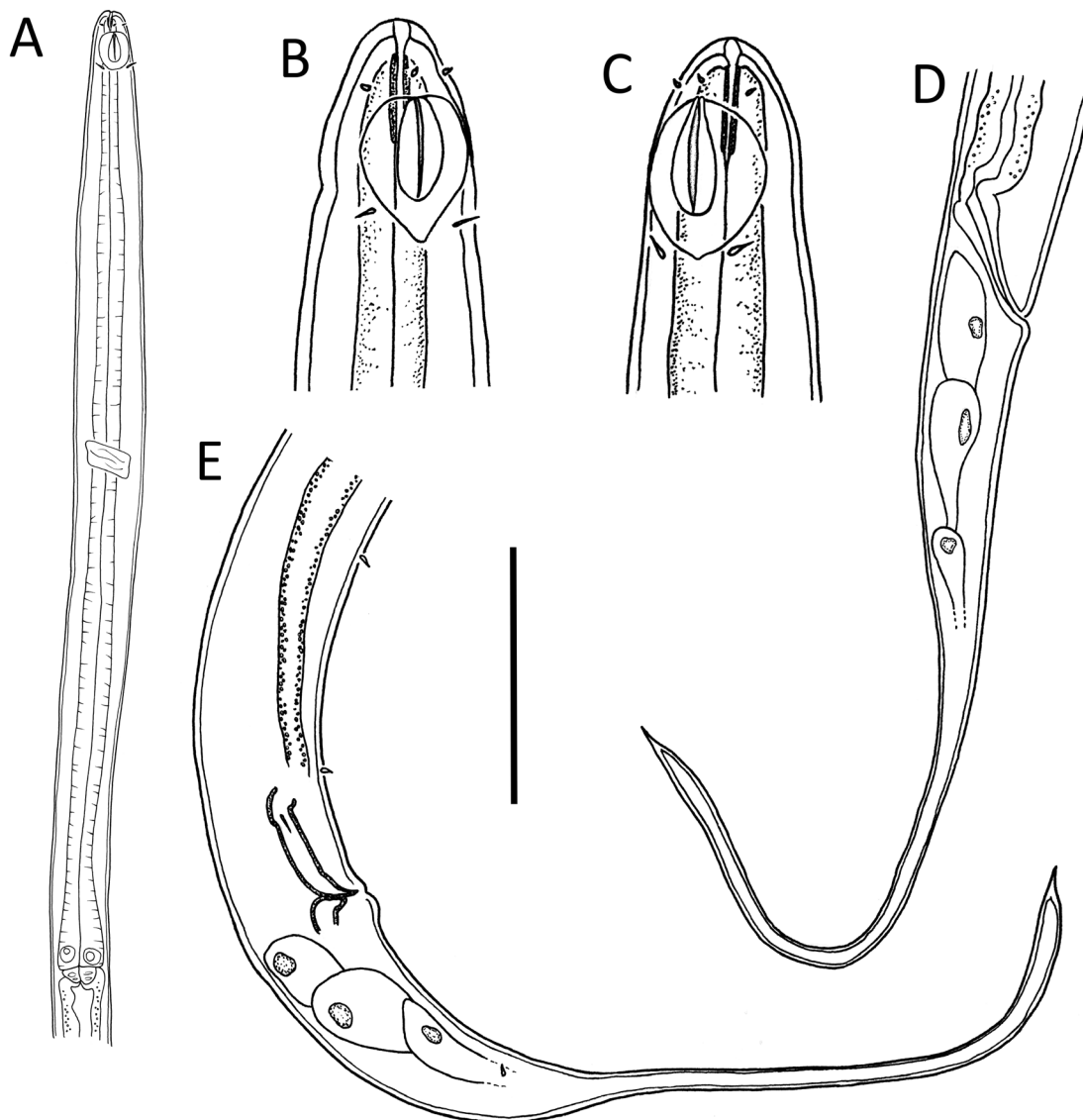


**Fig. 1.** *Litinium gludi* sp. nov. **A.** Anterior body region of the male holotype (NIWA 139257). **B.** Cephalic region of the female paratype (NIWA 139258). **C.** Cephalic region of the male paratype (NIWA 139258). **D.** Posterior body region of the female paratype (NIWA 139258). **E.** Posterior body region of the male holotype (NIWA 139257). Scale bar: A = 65  $\mu\text{m}$ , B–C = 15  $\mu\text{m}$ , D–E = 25  $\mu\text{m}$ .



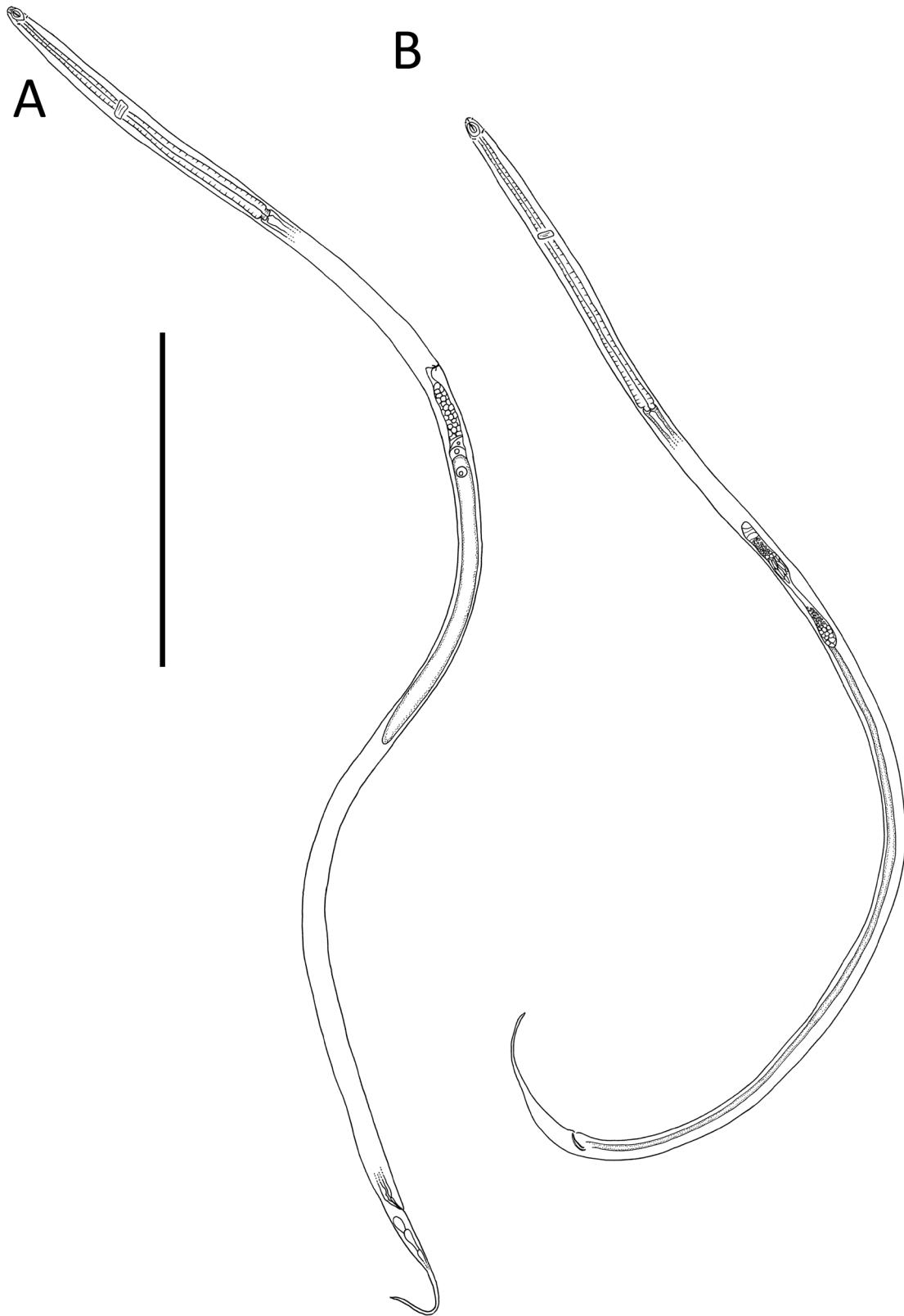


**Fig. 2.** *Litinium gludi* sp. nov. **A.** Entire female paratype (NIWA 139258). **B.** Entire male holotype (NIWA 139257). Scale bar = 200  $\mu$ m.

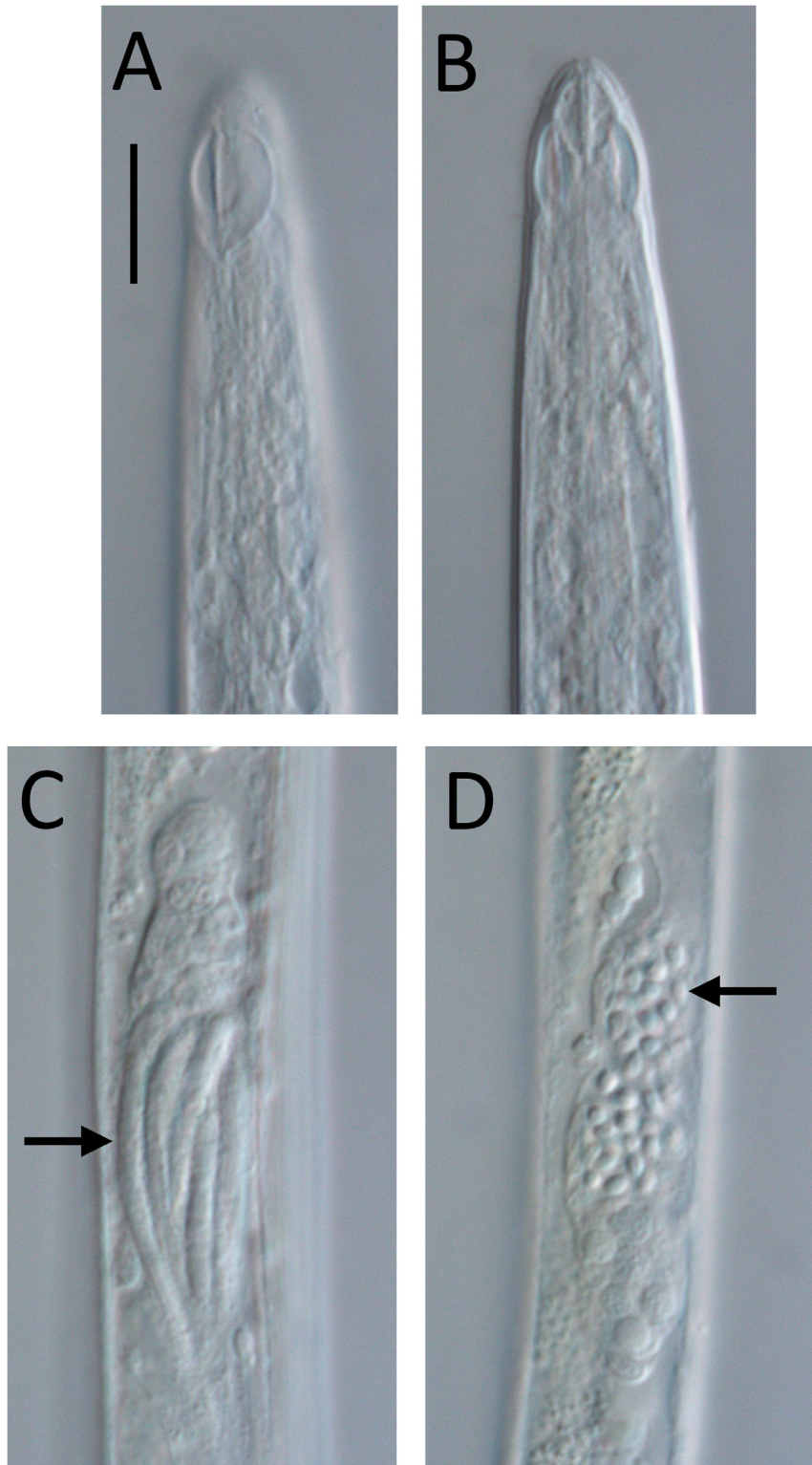


**Fig. 3.** *Litinium gludi* sp. nov., light micrographs of the male holotype (NIWA 139257). **A.** Surface view of cephalic region showing amphid and outer labial sensilla. **B.** Optical cross-section of cephalic region showing narrow buccal cavity and pharynx. **C.** Anterior testis showing elongated sperm cells (arrow). **D.** Posterior testis showing globular sperm cells (arrow). Scale bar = 10  $\mu$ m.

second precloacal papilla located 19–22  $\mu\text{m}$  from posterior-most precloacal papilla. Ejaculatory glands not observed. Tail conico-cylindrical, with pointed tip, caudal capsule absent; three caudal glands present posterior to cloaca; spinneret not observed.

#### **Female**

Similar to males but without any somatic setae on tail. Reproductive system with single posterior genital branch and reflexed ovary. Oocyte up to  $160 \times 10 \mu\text{m}$ . Vulva located far anteriorly at about  $\frac{1}{3}$  of body length from anterior extremity. Vagina perpendicular to body surface; vaginal glands not observed.

#### ***Molecular phylogenetic relationships***

Near full-length SSU (1516 bp) and D2-D3 of LSU sequences (756 bp) were obtained for *Litinium gludi* sp. nov. The Oxystominidae did not form a monophyletic clade in the consensus SSU tree due to the placement of *Rhaptothyerus typicus* Hope & Murphy, 1969 and oncholaimoid sequences among the oxystominid sequences (Fig. 5). Neither the Halalaiminae (represented by *Halalaimus* and *Oxystomina*) nor the Oxystomininae (all other oxystominid genera) were recovered as monophyletic. *Litinium*



**Fig. 4.** *Litinium gludi* sp. nov., light micrograph of tail tip of the male holotype (NIWA 139257), showing absence of caudal capsule and spinneret. Scale bar = 2  $\mu\text{m}$ .

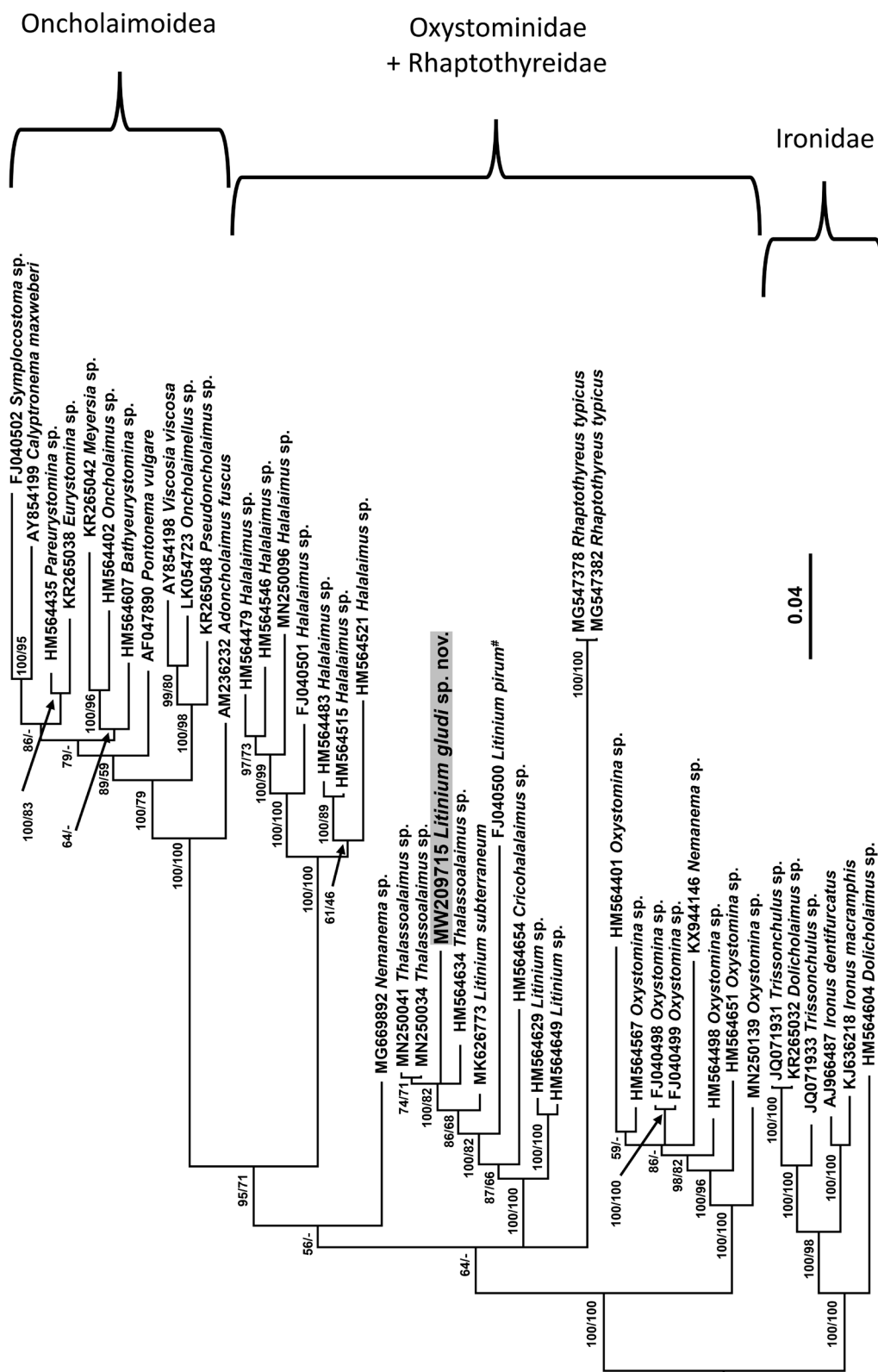


**Fig. 5.** Bayesian tree inferred from SSU sequences, aligned using the MUSCLE alignment algorithm under the general time-reversible (GTR) + I (proportion of invariable sites) + gamma distribution (G) model. The new sequence is shown in bold font on a grey background. Posterior probabilities (left) and bootstrap values (right) greater than or equal to 50% are given on appropriate clades. The scale stands for substitutions per site. - : less than 50% bootstrap support; #: sequence FJ040500 is labelled *Thalassoalaimus pirum* in GenBank but is labelled *Litinium pirum* here to reflect the new classification of this species proposed by Martelli *et al.* (2017).

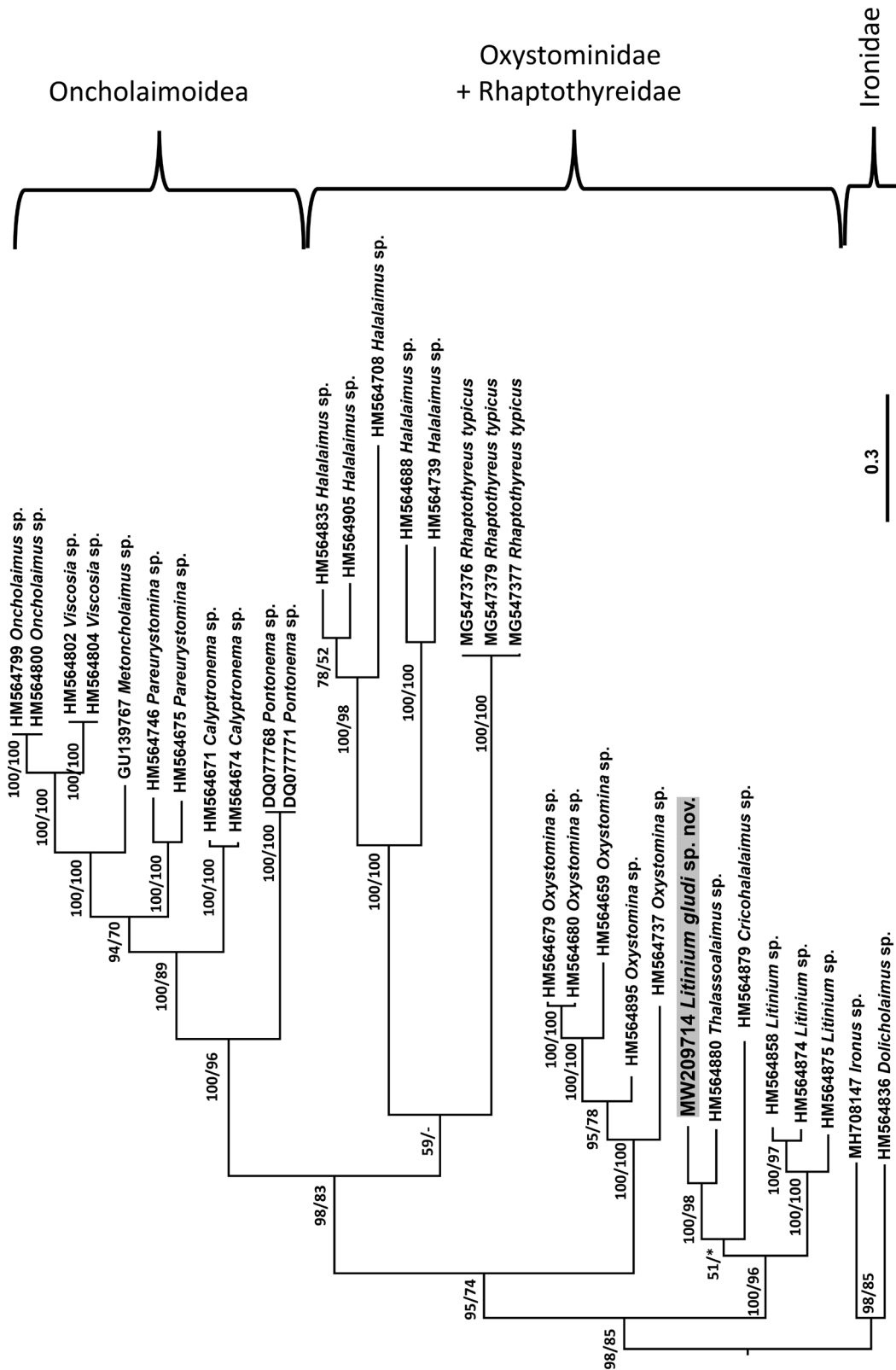


**Fig. 6.** Bayesian tree inferred from D2-D3 of LSU sequences, aligned using the MUSCLE alignment algorithm under the general time-reversible (GTR) + I (proportion of invariable sites) + gamma distribution (G) model. Posterior probabilities (left) and bootstrap values (right) greater than or equal to 50% are given on appropriate clades. The new sequence is shown in bold font on a grey background. The scale stands for substitutions per site. \* : no bootstrap support; - : less than 50% bootstrap support.

*gludi* sp. nov. was placed in a well-supported clade (100% posterior probability and 82% bootstrap support) with sequences of *Thalassoalaimus*. The similarity between SSU sequences of *Litinium gludi* sp. nov. and *Thalassoalaimus* sp. was 94–95% with a difference of 69 in 1508 nucleotides with 4 gaps (MN250034), 83 in 1504 nucleotides with 1 gap (HM564634) and 43 in 798 nucleotides with 1 gap (MN250041). The *Litinium gludi* sp. nov. + *Thalassoalaimus* clade was part of a wider, strongly supported oxystominid clade including all sequences of *Litinium* and *Cricohalalaimus* (100% posterior probability and bootstrap support), although neither *Litinium* nor *Thalassoalaimus* were monophyletic. The similarity between SSU sequences of *Litinium gludi* sp. nov. and *Litinium* sp. was 87–94% with a difference of 84 in 1513 nucleotides with 5 gaps (FJ040500), 116 in 1516 nucleotides with 3 gaps (HM564629), 113 in 1514 nucleotides with 2 gaps (HM564649), and 46 in 786 nucleotides with 1 gap (MK626773). Sequences of *Halalaimus* formed a strongly supported (100% posterior probability and bootstrap support) monophyletic sister group to the Oncholaimoidea Filipjev, 1916, the latter also forming a strongly supported monophyletic group (100% posterior probability and bootstrap support). The sequences of *Oxystomina* formed a strongly supported group (100% posterior probability and bootstrap support), however this genus was not monophyletic due to the inclusion of a sequence of *Nemanema* Cobb, 1920 in the clade. The placement of another sequence of *Nemanema* as a sister group to the *Halalaimus* + Oncholaimoidea clade was poorly supported (56% posterior probability and <50% bootstrap support).

The topology of the D2-D3 of LSU consensus tree was similar to that of the SSU tree, with the Oxystominidae again not recovered as monophyletic (Fig. 6). Sequences of *Halalaimus* and *Oxystomina* each formed strongly supported monophyletic clades (100% posterior probability and bootstrap support). As in the SSU tree, *Litinium*, *Cricohalalaimus*, and *Thalassoalaimus* formed a strongly supported clade (100% posterior probability and bootstrap support), with *Litinium gludi* sp. nov. most closely related to *Thalassoalaimus* (100% posterior probability and 98% bootstrap support). The similarity between LSU sequences of *Litinium gludi* sp. nov. and *Thalassoalaimus* sp. was 92% with a difference of 118 in 664 nucleotides with 7 gaps (HM564880); the similarity between LSU sequences of *Litinium gludi* sp. nov. and *Litinium* sp. was 71–72% with a difference of 188 in 671 nucleotides with 13 gaps (HM564858), 184 in 671 nucleotides with 12 gaps (HM564874) and 183 in 671 nucleotides with 13 gaps (HM564875).

## Discussion

The topologies of our SSU and D2-D3 of LSU trees are very similar to the phylogeny of Bik *et al.* (2010a), which recovered four sub-clades: Oncholaimoidea, *Thalassoalaimus* + *Cricohalalaimus* + *Litinium*, *Oxystomina*, and *Halalaimus*. Bik *et al.* (2010a) noted that *Halalaimus* was consistently recovered as a long-branch clade, which may have a destabilizing effect on the internal tree topology. The inclusion of *Rhaptothyreus typicus* in the present study, which was also recovered as a long-branch clade, may have had a similar destabilizing effect, and the placement of this taxon in relation to the Oxystominidae as well as wider Enoplida remains uncertain (Leduc *et al.* 2018). Molecular phylogenetic analyses have not yet provided support for the monophyly of the Oxystomininae or Halalaiminae (Bik *et al.* 2010a; present study).

The morphology of *Litinium gludi* sp. nov. is consistent with other species of *Litinium* due to the shape of the amphids, the posterior position of the cephalic setae and the lack of a caudal capsule. However, both SSU and LSU trees indicate that the new genus is most closely related to *Thalassoalaimus*. The latter genus is similar to *Litinium* in the structure and position of cephalic sensilla, but differs from *Litinium* in having a caudal capsule. It should be noted that most of the sequences of *Thalassoalaimus* in GenBank were not identified to the species level, and that given the recent changes in the definitions of *Litinium* and *Thalassoalaimus* (Tchesunov *et al.* 2014; Martelli *et al.* 2017), some or possibly all of the sequences of *Thalassoalaimus* from GenBank included in our phylogenetic analyses may in

fact belong to *Litinium* or vice versa. For example, the SSU sequence of *Thalassoalaimus pirum*, the only sequence of *Thalassoalaimus* identified to species level in GenBank, has since been transferred to *Litinium* by Martelli *et al.* (2017) (see Fig. 4). This uncertainty puts into question the apparent close relationship between the new species and *Thalassoalaimus* in molecular analyses. Therefore, given the current morphological definitions of *Litinium* and *Thalassoalaimus*, we choose to place the new species within *Litinium*, despite the apparently contradictory findings of molecular analyses.

Our phylogenetic analyses provide strong support for the placement of the new genus within a clade containing both *Thalassoalaimus* and *Litinium*, and within the Oxystomininae. Interestingly, the placement of *Cricohalalaimus* together with *Thalassoalaimus* and *Litinium* indicates that this genus, which is characterized by conflicting features used to define the Halalaiminae (elongated amphideal aperture) and Oxystomininae (female with single posterior ovary), should be placed within the Oxystomininae and not in the Halalaiminae as is currently the case (Smol *et al.* 2014). An analogous change to the classification of the *Rhabdocoma* Cobb, 1920 (Enoplida, Trefusiidae Gerlach, 1966 (De Ley & Blaxter 2004)) was suggested by Shi & Xu (2017), who found that SSU phylogenetic relationships supported the classification of this genus with the Halononchinae Wieser & Hopper, 1967, a classification consistent with variation in the structure of the female reproductive system, and not in the Trefusiinae Gerlach, 1966, as previously suggested based on buccal morphology. Similarly, in the case of *Cricohalalaimus*, it appears that the shape of the amphideal aperture is not as informative as the structure of the female reproductive system for subfamily-level classification, and we therefore propose that *Cricohalalaimus* be moved to the Oxystomininae.

## Acknowledgments

We thank the co-voyage leaders Ronnie N. Glud and Ashley A. Rowden and science party of voyage TAN1711, and the officers and crew of *RV Tangaroa* for their contribution to sample collection. The voyage was funded by European Research Council Advanced Grant (ERC adG 2014 grant agreement number 669947) as part of the HADES-ERC trench project, with additional support from various national research programmes. Funding for DL's participation in the voyage, and for the taxonomic analyses, was provided by NIWA's Coasts and Oceans Centre Research Programme 'Marine Biological Resources'. ZZ was supported by core funding for Crown Research Institutes from the Ministry of Business, Innovation and Employment's Science and Innovation Group. We are grateful to Megan Carter (NIWA) for processing the meiofauna samples and Duckchul Park (Landcare Research) for obtaining the molecular sequences. We thank two anonymous reviewers for providing constructive criticisms on the manuscript.

## References

- Allgén C.A. 1933. Freilebende Nematoden aus dem Trondhjemsfjord. *Capita Zoologica* 4: 1–162.
- Bik H.M., Lamshead P.J.D., Thomas W.K. & Hunt D.H. 2010a. Moving towards a complete molecular framework of the Nematoda: a focus on the Enoplida and early branching clades. *BMC Evolutionary Biology* 10: 353. <https://doi.org/10.1186/1471-2148-10-353>
- Bik H.M., Thomas W.K., Hunt D.H. & Lamshead P.J.D. 2010b. Low endemism, continued deep-shallow interchanges, and evidence for cosmopolitan distributions in free-living nematodes (order Enoplida). *BMC Evolutionary Biology* 10: 389. <https://doi.org/10.1186/1471-2148-10-389>
- De Ley P. & Blaxter M.L. 2004. A new system for Nematoda: combining morphological characters with molecular trees, and translating clades into ranks and taxa. *Nematology Monographs & Perspectives* 2: 633–653.

- Edgar R.C. 2004a. MUSCLE: multiple sequence alignment with high accuracy and high throughput. *Nucleic Acids Research* 32: 1792–1797. <https://doi.org/10.1093/nar/gkh340>
- Edgar R.C. 2004b. MUSCLE: a multiple sequence alignment method with reduced time and space complexity. *BMC Bioinformatics* 5: 113. <https://doi.org/10.1186/1471-2105-5-113>
- Gambi C., Vanreusel A. & Danovaro R. 2003. Biodiversity of nematode assemblages from deep-sea sediments of the Atacama Slope and Trench (South Pacific Ocean). *Deep Sea Research Part I: Oceanographic Research Papers* 50 (1): 103–117. [https://doi.org/10.1016/S0967-0637\(02\)00143-7](https://doi.org/10.1016/S0967-0637(02)00143-7)
- Guindon S., Dufayard J.F., Lefort V., Anisimova M., Hordijk W. & Gascuel O. 2010. New algorithms and methods to estimate Maximum-Likelihood phylogenies: Assessing the performance of PhyML 3.0. *Systematic Biology* 59: 307–321. <https://doi.org/10.1093/sysbio/syq010>
- Holterman M., van der Wurff A., van den Elsen S., van Megen H., Bongers T., Holovachov O., Bakker J. & Helder J. 2006. Phylum-wide analysis of SSU rDNA reveals deep phylogenetic relationships among nematodes and accelerated evolution toward crown clades. *Molecular Biology and Evolution* 23: 1792–1800. <https://doi.org/10.1093/molbev/msl044>
- Kearse M., Moir R., Wilson A., Stones-Havas S., Cheung M., Sturrock S., Buxton S., Cooper A., Markowitz S., Duran C., Thierer T., Ashton B., Meintjes P. & Drummond A. 2012. Geneious basic: an integrated and extendable desktop software platform for the organization and analysis of sequence data. *Bioinformatics* 28: 1647–1649. <https://doi.org/10.1093/bioinformatics/bts199>
- Leduc D. 2015. One new genus and five new nematode species (Monhysterida, Xyalidae) from Tonga and Kermadec Trenches, Southwest Pacific. *Zootaxa* 3964: 501–525. <https://doi.org/10.11646/zootaxa.3964.5.1>
- Leduc D. 2016. One new genus and three new species of deep-sea nematodes (nematoda: Microlaimidae) from the Southwest Pacific Ocean and Ross Sea. *Zootaxa* 4079: 255–271. <https://doi.org/10.11646/zootaxa.4079.2.7>
- Leduc D., Zhao Z.Q., Verdon V. & Xu Y. 2018. Phylogenetic position of the enigmatic deep-sea nematode order Rhaptothyreida: A molecular analysis. *Molecular Phylogenetics and Evolution* 122: 29–36. <https://doi.org/10.1016/j.ympev.2018.01.018>
- Lorenzen S. 1981. Entwurf eines phylogenetischen Systems der freilebenden Nematoden. *Veröffentlichungen des Instituts für Meeresforschung in Bremerhaven* 7: 1–472.
- Martelli A., Lo Russo V., Villares G. & Pastor de Ward C.T. 2017. Two new species of free-living marine nematodes of the family Oxystominidae Chitwood, 1935 (Enoplida) with a review of the genus *Thalassoalaimus* de Man, 1893 from the Argentine coast. *Zootaxa* 4250: 347–357. <https://doi.org/10.11646/zootaxa.4250.4.5>
- Miljutin D.M., Gad G., Miljutina M.M., Mokievsky V.O., Fonseca-Genevois V. & Esteves A.M. 2010. The state of knowledge on deep-sea nematode taxonomy: how many valid species are known down there? *Marine Biodiversity* 40: 143–159. <https://doi.org/10.1007/s12526-010-0041-4>
- Nunn G.B. 1992. *Nematode Molecular Evolution*. PhD Thesis, University of Nottingham, UK.
- Nylander J.A.A. 2004. MrModeltest. Ver. 2. Program distributed by the author. Evolutionary Biology Centre, Uppsala University. Available from <https://github.com/nylander/MrModeltest2> [accessed 8 Apr. 2021].
- Rambaut A. & Drummond A.J. 2007. Tracer. Ver. 1.4. Available from <http://beast.community/tracer> [accessed 8 Apr. 2021].



Shi B. & Xu K. 2017. Morphological and molecular characterizations of *Africanema multipapillatum* sp. nov. (Nematoda, Enoplida) in intertidal sediment from the East China Sea. *Marine Biodiversity* 48: 281–288. <https://doi.org/10.1007/s12526-017-0690-7>

Somerfield P.J. & Warwick R.M. 1996. *Meiofauna in Marine Pollution Monitoring Programmes: a Laboratory Manual*. Lowestoft, Ministry of Agriculture, Fisheries and Food.

Smol N., Muthumbi A. & Sharma J. 2014. Order Enoplida. In: Schmidt-Rhaesa A. (ed.) *Handbook of Zoology: Gastrotricha, Cycloneuralia and Gnathifera. Volume 2: Nematoda*: 193–249. De Gruyter, Berlin.

Swofford D.L. 2002. PAUP\*. Phylogenetic Analysis Using Parsimony (and Other Methods). Ver. 4. Sinauer Associates, Sunderland.

Tchesunov A.V., Thanh N.V. & Tu N.D. 2014. A review of the genus *Litinium* Cobb, 1920 (Nematoda: Enoplida: Oxystominidae) with descriptions of four new species from two contrasting habitats. *Zootaxa* 3872: 57–76. <https://doi.org/10.11646/zootaxa.3872.1.5>

Zheng J.W., Subbotin S.A., He S.S., Gu J.F. & Moens M. 2002. Molecular characterisation of some Asian isolates of *Bursaphelenchus xylophilus* and *B. mucronatus* using PCR RFLPs and sequences of ribosomal DNA. *Russian Journal of Nematology* 11: 17–22.

*Manuscript received: 29 November 2020*

*Manuscript accepted: 9 February 2021*

*Published on: 7 May 2021*

*Topic editor: Rudy Jocqué*

*Desk editor: Natacha Beau*

Printed versions of all papers are also deposited in the libraries of the institutes that are members of the *EJT* consortium: Muséum national d'histoire naturelle, Paris, France; Meise Botanic Garden, Belgium; Royal Museum for Central Africa, Tervuren, Belgium; Royal Belgian Institute of Natural Sciences, Brussels, Belgium; Natural History Museum of Denmark, Copenhagen, Denmark; Naturalis Biodiversity Center, Leiden, the Netherlands; Museo Nacional de Ciencias Naturales-CSIC, Madrid, Spain; Real Jardín Botánico de Madrid CSIC, Spain; Zoological Research Museum Alexander Koenig, Bonn, Germany; National Museum, Prague, Czech Republic.